Submitted to the J. of Electrochemical Society

UCRL-18798
Preprint

cy. 2

RECEIVED
LAWRENCE
RADIATION LABORATORY
APR 2 2 1969
LIBRARY AND
DOCUMENTS SECTION

CURRENT DISTRIBUTIONS ON PLANE, PARALLEL ELECTRODES IN CURRENT FLOW

W. R. Parrish and John Newman

March 1969

AEC Contract No. W-7405-eng-48

TWO-WEEK LOAN COPY

This is a Library Circulating Copy which may be borrowed for two weeks. For a personal retention copy, call Tech. Info. Division, Ext. 5545

UCRL-18798
cy. 2

LAWRENCE RADIATION LABORATORY
UNIVERSITY of CALIFORNIA BERKELEY

DISCLAIMER

This document was prepared as an account of work sponsored by the United States Government. While this document is believed to contain correct information, neither the United States Government nor any agency thereof, nor the Regents of the University of California, nor any of their employees, makes any warranty, express or implied, or assumes any legal responsibility for the accuracy, completeness, or usefulness of any information, apparatus, product, or process disclosed, or represents that its use would not infringe privately owned rights. Reference herein to any specific commercial product, process, or service by its trade name, trademark, manufacturer, or otherwise, does not necessarily constitute or imply its endorsement, recommendation, or favoring by the United States Government or any agency thereof, or the Regents of the University of California. The views and opinions of authors expressed herein do not necessarily state or reflect those of the United States Government or any agency thereof or the Regents of the University of California.

UCRL-18798

Current Distributions on Plane, Parallel Electrodes in Channel Flow

W. R. Parrish and John Newman

Inorganic Materials Research Division,
Lawrence Radiation Laboratory, and
Department of Chemical Engineering
University of California, Berkeley

March 1969

Abstract

Current distributions on two plane, parallel electrodes embedded in the walls of a flow channel have been calculated for separation distance between electrodes to electrode length ratios of 0.5, 1, and 10. Secondary current distributions were calculated using the linear and Tafel polarization laws. Using the Tafel polarization law, current distributions were calculated at various fractions of the limiting current. In all cases considered, the electrodes are nearly independent of one another if the height to length ratio is ten or more.

Introduction

Many industrial electrochemical processes use channel flow between two plane, parallel electrodes as shown in figure 1. The limiting current distribution for this flow geometry is well known[1]. A procedure for determining current distributions below the limiting current has been outlined previously[1]. The method uses the concept of having concentration variations restricted to a thin diffusion layer very near each electrode surface[2], allowing the bulk region and the diffusion layers to be treated separately. The same concept has been applied previously to the rotating disk electrode[3,4] and to the single plane electrode[5].

In the treatment of the problem, the following assumptions are made:

1. The electrodes are embedded in infinite, parallel, plane, insulating walls.

2. Fully developed, laminar flow exists, and the velocity profile can be considered linear inside the diffusion layer.

3. Dilute-solution theory with constant physical properties is applicable.

4. The transport equations used here apply to either single salt deposition or ions reacting in an excess of supporting electrolyte. The effect of ionic migration for intermediate cases is not considered.

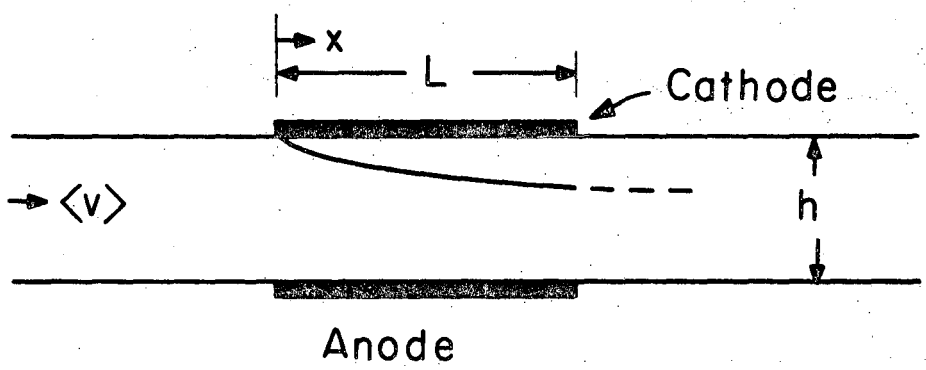

Figure 1. Plane electrodes in the walls of a flow channel

XBL673-2382A

Mathematical Formulation of Problem

The general approach to the problem is outlined in references 1 through 5. The potential in the bulk region satisfies Laplace's equation:

$$\frac{\partial^2\Phi}{\partial x^2} + \frac{\partial^2\Phi}{\partial y^2} = 0 \quad , \tag{1}$$

where Φ is the potential measured by a reference electrode of the same type as the working electrode. The appropriate boundary conditions are:

$$\partial\Phi/\partial y = 0 \text{ at } y = 0 \text{ and } y = h \text{ for } x < 0 \text{ and } x > L \quad , \tag{2}$$

$$\partial\Phi/\partial y = -i/\kappa_\infty \text{ at } y = 0 \text{ and } y = h \text{ for } 0 < x < L \quad . \tag{3}$$

Equation 2 applies to the insulating surfaces bounding the electrodes, and equation 3 relates the normal potential gradient to the electrode current density i, where κ_∞ is the solution conductivity in the bulk region. The current is taken to be positive on the anode and negative on the cathode.

The solution[1] to equation 1 with the boundary conditions is:

$$\Phi(x,y) = \Phi^* - \frac{1}{2\pi\kappa_\infty}\left\{\int_0^L i_{cath}(x')\ln[\sinh^2(\pi(x-x')/2h) + \sin^2(\pi(y-h)/2h)]dx' + \int_0^L i_{anode}(x')\ln[\sinh^2(\pi(x-x')/2h) + \sin^2(\pi y/2h)]dx'\right\}, \tag{4}$$

where the anode is at y = 0 and the cathode is at y = h. The potential very near the cathode surface is then

$$\Phi^{o}_{cath}(x) = \Phi^{*} - \frac{1}{2\pi\,\kappa_{\infty}}\left\{\int_{o}^{L}[i_{cath}(x')\ln\ \sinh^{2}(\pi(x-x')/2h)\right.$$

$$\left. + i_{anode}(x')\ln\cosh^{2}\ (\pi(x-x')/2h)]dx'\right\} \quad . \tag{5}$$

The expression for the anodic potential is the same as above except that the subscripts are reversed. These potentials represent the potentials of the bulk region extrapolated to the electrode surface as if the actual current prevails but there is no concentration variation near the electrodes. The integration constant, Φ^{*}, is determined by the requirement that the total currents for the two electrodes must be equal in magnitude, i.e.,

$$\int_{o}^{L}[i_{cath}(x') + i_{anode}(x')]dx' = 0 \quad . \tag{6}$$

To obtain a relationship between the current and concentration on each electrode, an equation has been derived from the limiting current expression

$$i(x) = -\frac{nFD}{(1-t)}\,\frac{c_{\infty}}{\Gamma(4/3)}\left(\frac{2\langle v\rangle}{3hDx}\right)^{1/3} \quad . \tag{7}$$

Application of Duhamel's theorem[6] yields an equation which is applicable to either electrode[1]:

$$i(x) = \frac{nFD}{(1-t)\Gamma(4/3)}\left(\frac{2\langle v\rangle}{3hD}\right)^{1/3}\int_{o}^{x}\frac{dc_{o}(x')}{dx'}\,\frac{dx'}{(x-x')^{1/3}} \quad . \tag{8}$$

For many electrode reactions, the current density and surface overpotential, η_s, can be related by

$$i(x) = i_o(c_o/c_\infty)^\gamma \left\{\exp[\alpha ZF\eta_s/RT] - \exp[-\beta ZF\eta_s/RT]\right\} \quad , \tag{9}$$

where α and β are characteristic parameters of the electrode reaction and i_o is the exchange current density at the bulk concentration. The exchange current density is assumed to be proportional to the surface concentration, c_o, raised to the power γ. The surface overpotential on each electrode is related to the electrode potential, V, by

$$\eta_s = V - \Phi^o - \eta_c \quad . \tag{10}$$

The concentration overpotential, η_c, is taken to be[2]

$$\eta_c = -(RT/ZF)[\ln(c_\infty/c_o) - t(1-c_o/c_\infty)] \quad , \tag{11}$$

where

$$Z = -z_+z_-/(z_+-z_-) \text{ for a single salt} \quad , \tag{12}$$

$$Z = -n \text{ with supporting electrolyte} \quad . \tag{13}$$

The transference number, t, is zero if there is an excess of supporting electrolyte. The number Z was inserted into equation 9 in order to make more simple the dimensionless parameters which describe the system. The kinetic parameters are αZ and βZ, not α and β alone.

Numerical Calculations

To calculate current and concentration distributions on the two electrodes, two sets of five equations must be solved simultaneously; these are equations 5, 8, 9, 10, and

$$i_{avg} = \left| \int_0^L i(x)dx \right| \quad . \tag{14}$$

i_{avg} is a specified average current density applying to both electrodes (equation 14 replaces equation 6). For a given distribution of total overpotential, $\eta_c + \eta_s$, equation 8 was solved in conjunction with equations 9 and 10 using the method of Acrivos and Chambré[7]. Simpson's method was used to evaluate equation 14. Gaussian quadrature integration, using 96 points[8], was used to calculate the total overpotential in equation 5. To get intermediate values of the integrand required for the Gaussian integration, Lagrange's interpolation formula was used. Simpson's method had been used for evaluating equation 5 but was found to be less accurate and efficient than the Gaussian method. The singularity at $x' = x$ in equation 5 was eliminated by adding and subtracting $i(x)$ as suggested by Kantorovich and Krylov[9].

The answers were considered satisfactory if they did not change by more than one percent when the number of evenly spaced intervals was increased by 20. The required number of intervals varied between 100 and 180, depending upon the uniformity of the current and concentration distributions.

The following doubly reiterative procedure was used:

1. As a first guess, the total overpotential was assumed constant over the entire electrode. The overpotentials were calculated from equation 9 using $i(x) = i_{avg}$ and $c_o = c_\infty$.

2. For a given overpotential distribution, the current and concentration distributions were calculated from equations 8, 9, 10, and 11.

3. The average current was then calculated and compared with i_{avg}. If the two values differed by more than 0.001%, the overpotential distribution was changed uniformly by adding a constant to each value. The new overpotentials were then put back into step 2. The constant was found by assuming that the overpotential at $x = 0$ was proportional to the calculated average current density or its logarithm for the cathode or the anode, respectively.

4. Using the current distributions that satisfy equation 14, new values of the overpotentials were calculated from equations 5 and 10. If the old and new values differed by more than 0.1%, the two values were averaged (usually with unequal weights because of stability problems) and put back into step 2.

This numerical procedure works well for the range of current distributions considered in this paper. Three to eight iterations were required to obtain convergence in the inner loop, and the convergence rate depended upon how near the overpotential distributions were to the "correct" values. Up to 70 iterations were required in the outer loop. The required number of outer iterations increased with increasing nonuniformity of the current and concentration distributions.

Results

Eight parameters are required to define completely each problem-- h/L, the transference number, t, α, β, and γ which are characteristic of the electrode reaction (although it is not necessary, the same kinetic parameters are assumed to apply to both electrodes) and three dimensionless quantities which are analogous to those defined for the flat plate[5] and the rotating disk[3] electrodes:

$$J = ZFLi_o/RT\kappa_\infty \quad , \tag{15}$$

$$N = \frac{nZF^2Dc_\infty}{(1-t)RT\kappa_\infty}\left(\frac{6\langle v\rangle L^2}{hD}\right)^{1/3} \quad , \tag{16}$$

$$\delta = \left|i_{avg}\right| ZFL/RT\kappa_\infty \quad , \tag{17}$$

where J, N, and δ represent the dimensionless exchange, average limiting, and average current densities. The average limiting current corresponds to $\delta = 0.807\ N$.

The two extreme cases are the primary and limiting current distributions which are shown in figure 2 for several values of h/L. The primary current distribution occurs when the electrode is reversible and there are no concentration effects ($N = \infty$, $J = \infty$). The primary current distribution[1] is

$$i/i_{avg} = \frac{\epsilon \cosh \epsilon/K(\tanh^2\epsilon)}{\sqrt{\sinh^2\epsilon \ \sinh^2(2x-L)\epsilon/L}} \quad , \tag{18}$$

where $\epsilon = \pi L/2h$ and $K(m)$ is the complete elliptic integral of the first kind.

The limiting current occurs when the current distribution is limited by the mass transfer rate through the diffusion layer and is given by

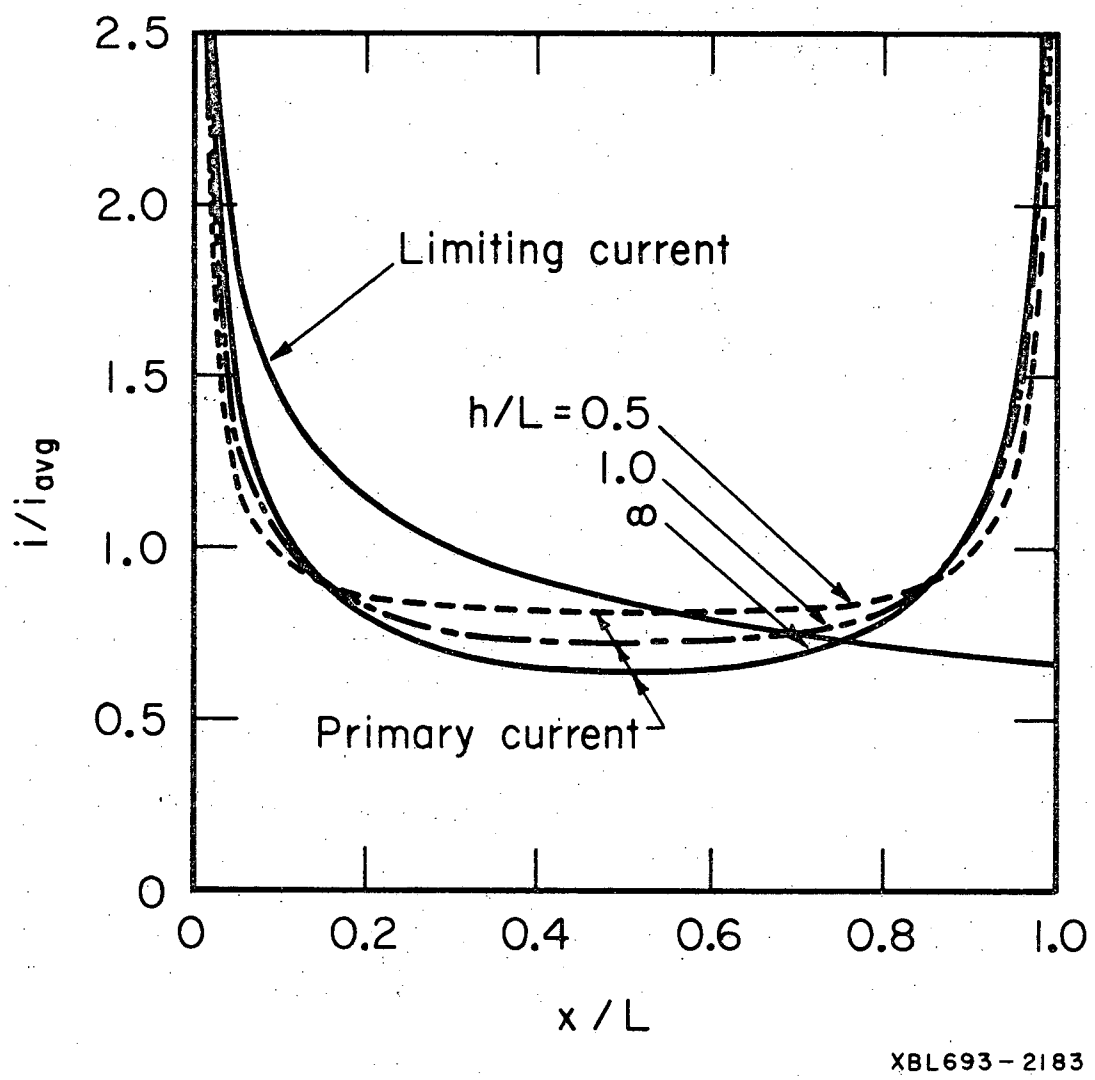

Figure 2. Primary and limiting current distribution on channel electrodes.

$$i/i_{avg} = (2/3)\ (x/L)^{-1/3} \quad . \tag{19}$$

Secondary current distributions occur when there is a surface overpotential but no mass transfer effects ($N=\infty$). If the current density is small ($\delta \ll J$), the polarization law 9 can be linearized to give

$$i = (\alpha+\beta)(ZF/RT)i_o\eta_s \quad . \tag{20}$$

Using the coefficient in equation 20 (which, after multiplication by L/κ_∞, becomes $(\alpha+\beta)J$) as a parameter, Wagner[10] calculated secondary current distributions for the two cases of $h/L = \infty$ and $h/L \ll 1$. Linear secondary current distributions are shown in figure 3 for $(\alpha+\beta)J$ equal to 8π (this corresponds to Wagner's parameter $a/k_c = 4\pi$) and several values of h/L. To give an indication of current uniformity, the ratio of the maximum to minimum current density has been plotted in figure 4 as a function of $(\alpha+\beta)J$ and h/L.

If the average current is much greater than the exchange current ($\delta \gg J$), Tafel polarization will apply. Equation 9 can then be written as

$$\eta_s = -(RT/ZF\beta)[\ln|i|-\ln i_o] \quad , \tag{21}$$

for the cathode. (For the anode, α replaces β and the minus sign is omitted.) Poddubnyĭ, Rudenko, and Formin[11] have calculated secondary current distributions for Tafel polarization and $h/L = \infty$. Figures 5 and 6 show current distributions and current uniformity curves for Tafel kinetics.

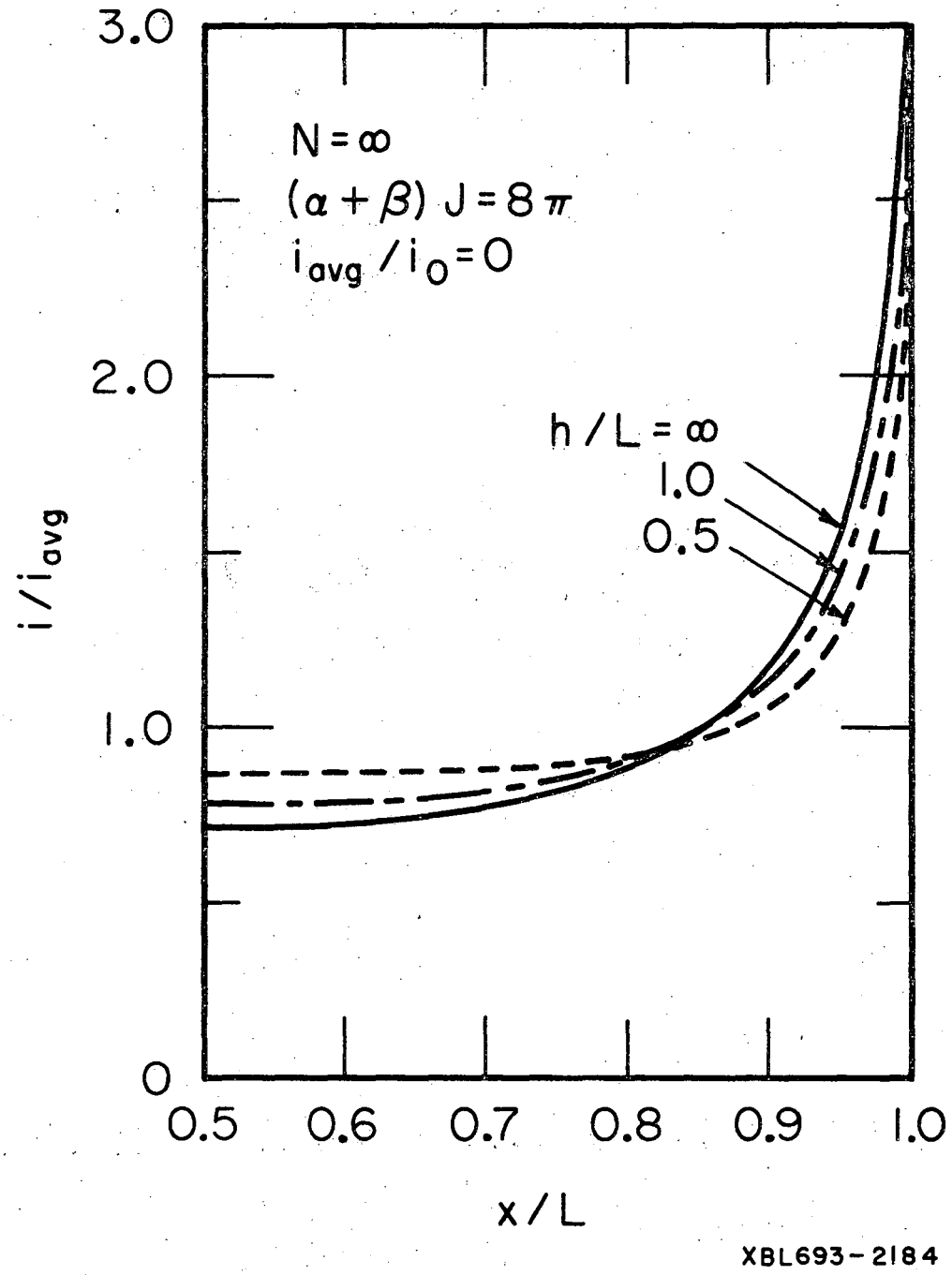

Figure 3. Secondary current distribution for linear polarization.

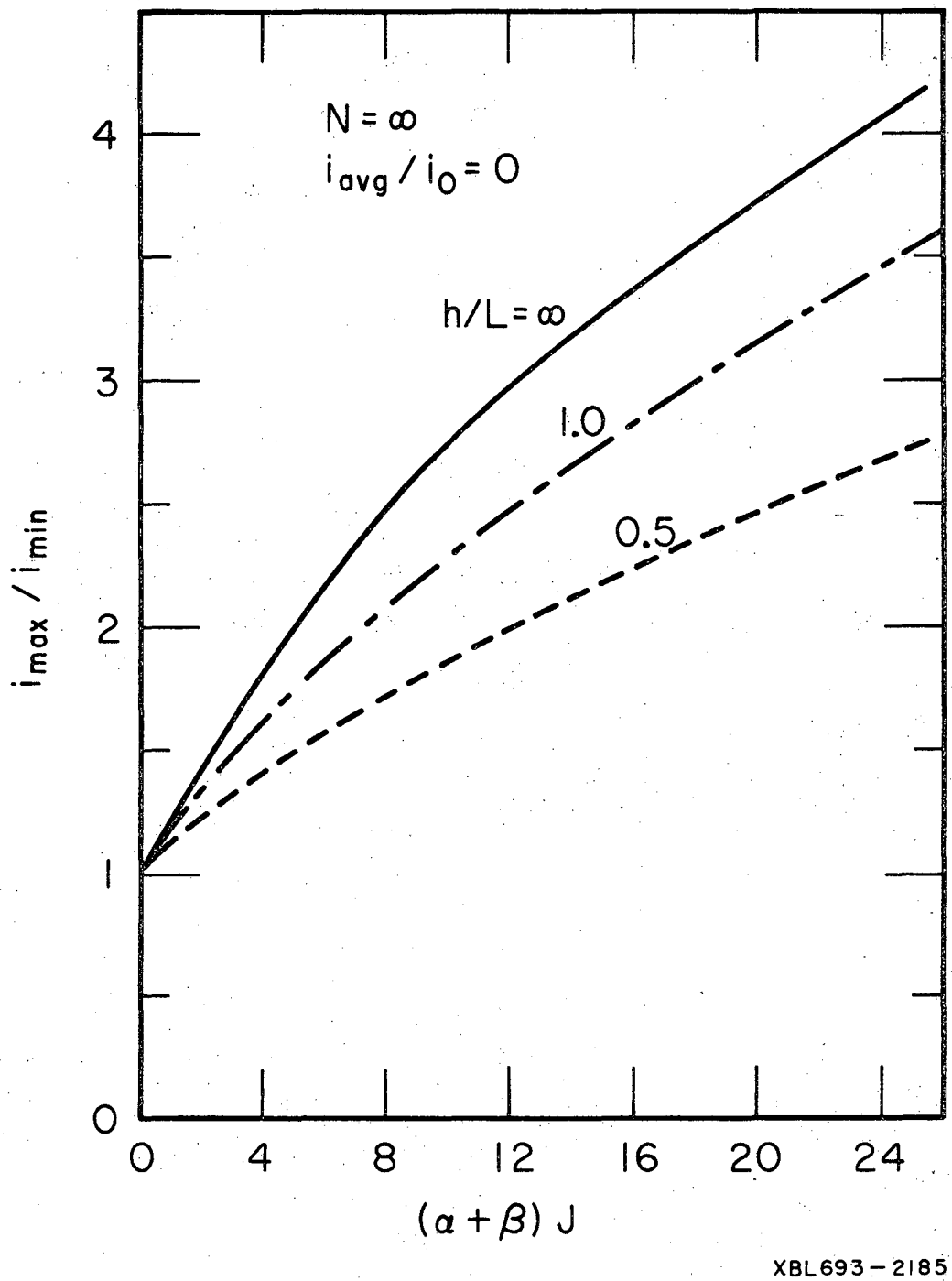

Figure 4. Ratio of maximum to minimum current for linear polarization as a function of the parameter $(\alpha+\beta)J$.

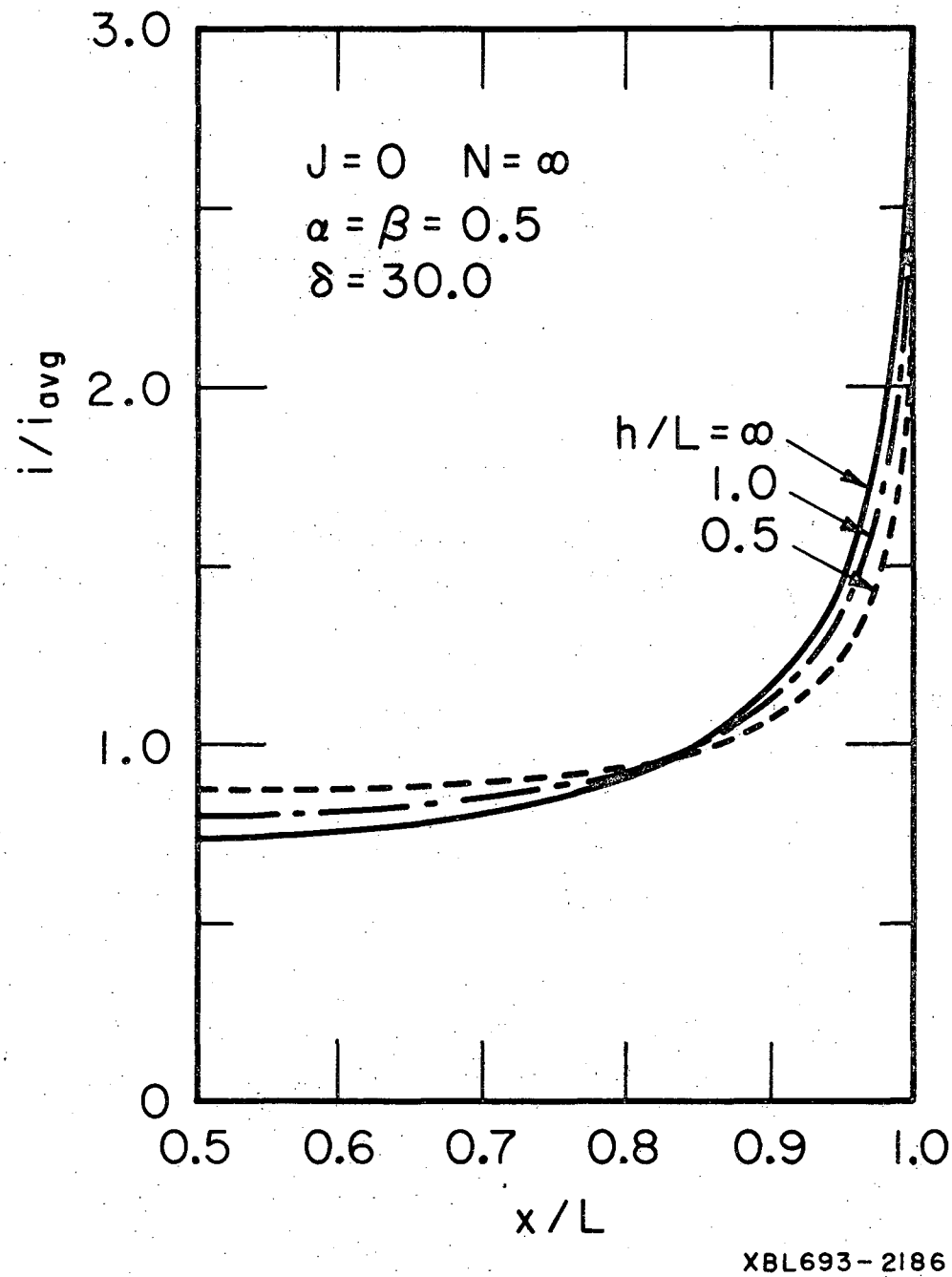

Figure 5. Current distribution for Tafel polarization.

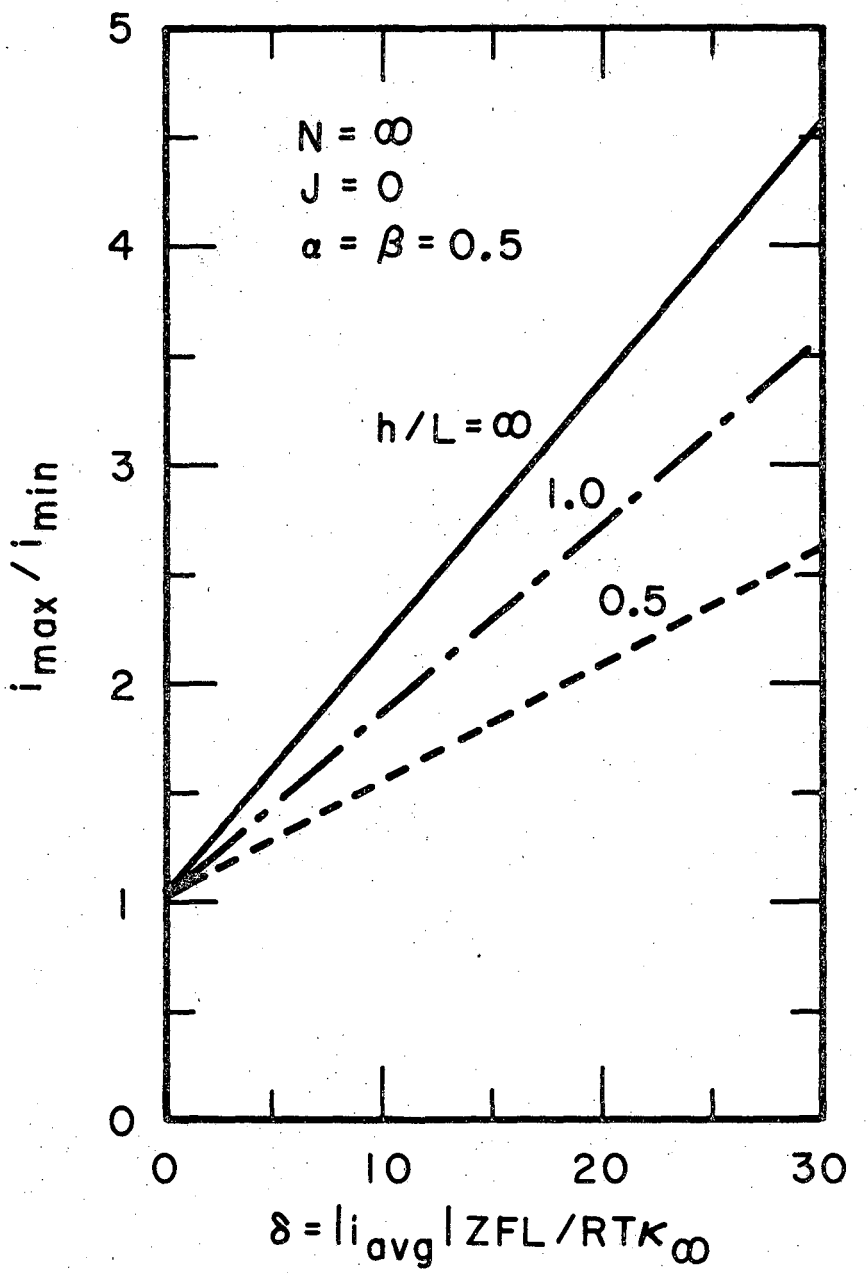

XBL693-2187

Figure 6. Ratio of maximum to minimum current for Tafel polarization with no mass transfer effects as a function of the dimensionless average current.

As can be seen in figures 3 through 6, the current distributions become increasingly more sensitive to h/L as the ratio decreases. For all the cases considered, the current distributions for h/L = 10 were very close to the distributions for h/L = ∞.

Because mass transfer effects are important at higher current densities, we used Tafel polarization in calculating current distributions involving concentration effects. Figure 7 shows the current distribution on the cathode at various fractions of the limiting current and for three values of h/L. The current distribution on the anode is shown in figure 8 for a current which is 95 percent of the limiting current. Near the front of each electrode, the current drops rapidly, behaving like a secondary current distribution. However, on the cathode, mass transfer effects become more important with increasing x/L. As the concentration profiles for the cathode show in figure 9, the cathodic current cannot continue to behave like a secondary current because the reactant concentration has been lowered inside the diffusion layer. But concentration effects are relatively unimportant on the anode, and the anodic current continues to resemble a secondary current distribution. The interaction between the two electrodes through Laplace's equation is very apparent for the case of h/L = 0.5.

For the cathode, at higher current densities, the concentration drops rapidly at the front of the electrode and, as x/L increases, the concentration increases slightly before decreasing again for h/L equal to 1.0 or more. This behavior is caused by the rapid depletion of reactant at the beginning when the current density is very high. However, after the current has dropped, the concentration has a chance to increase by diffusion into the diffusion layer. Then, when the current increases, the concentration starts decreasing again. A similar but opposite behavior occurs on the anode as is shown in figure 10.

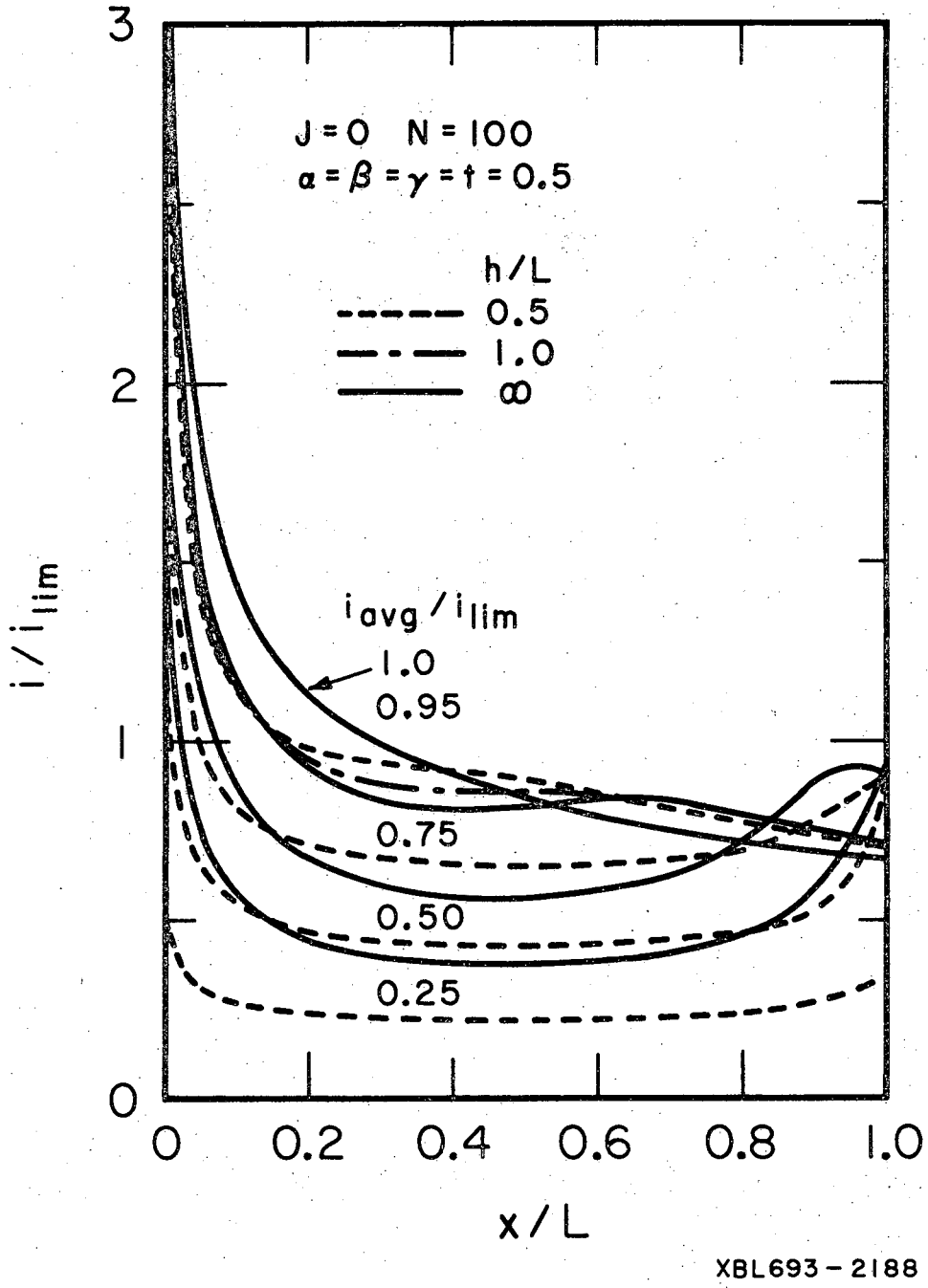

Figure 7. Current distribution on the cathode for Tafel polarization near the limiting current.

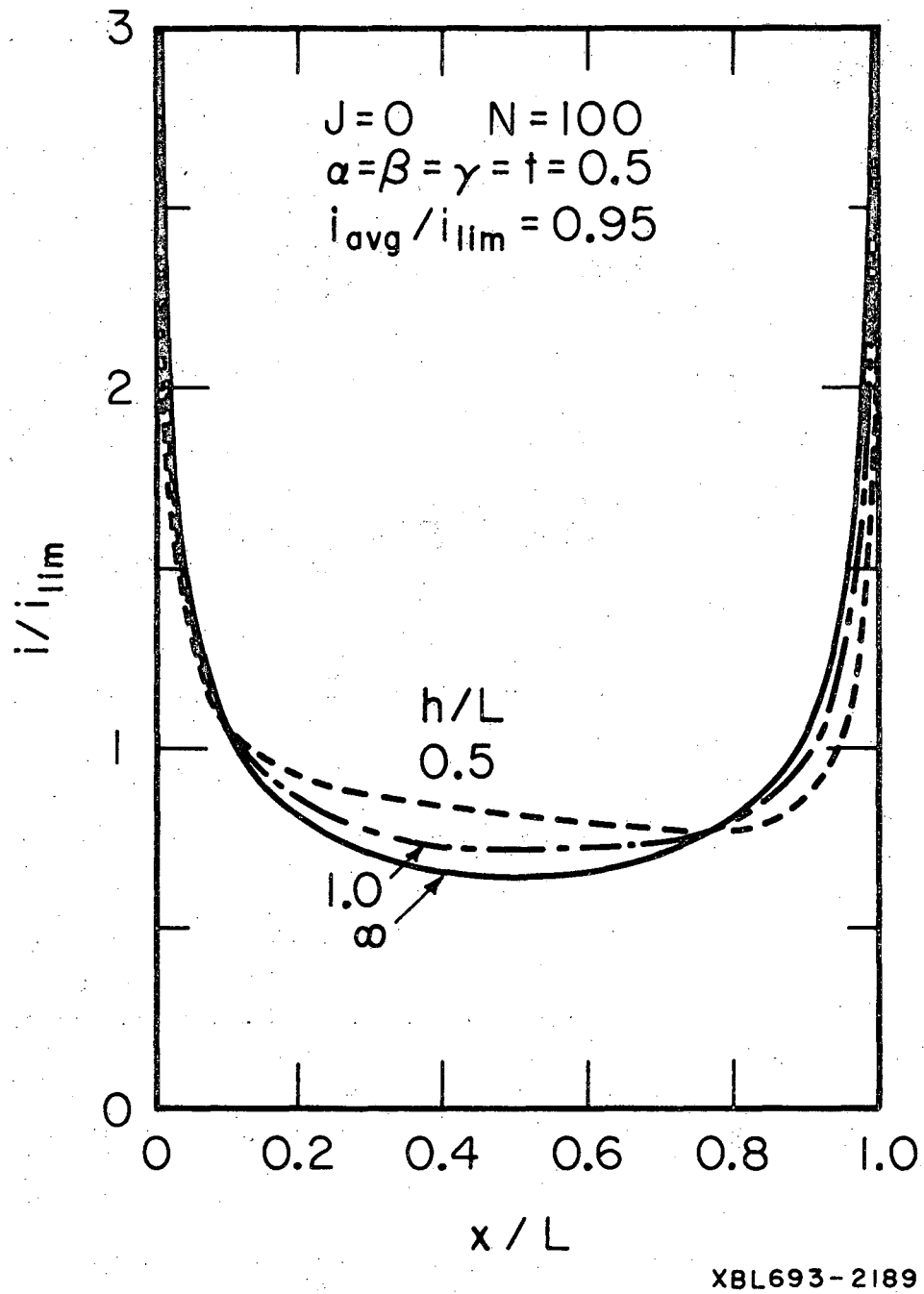

Figure 8. Current distribution on the anode for Tafel polarization with the current at 95 per cent of the limiting current.

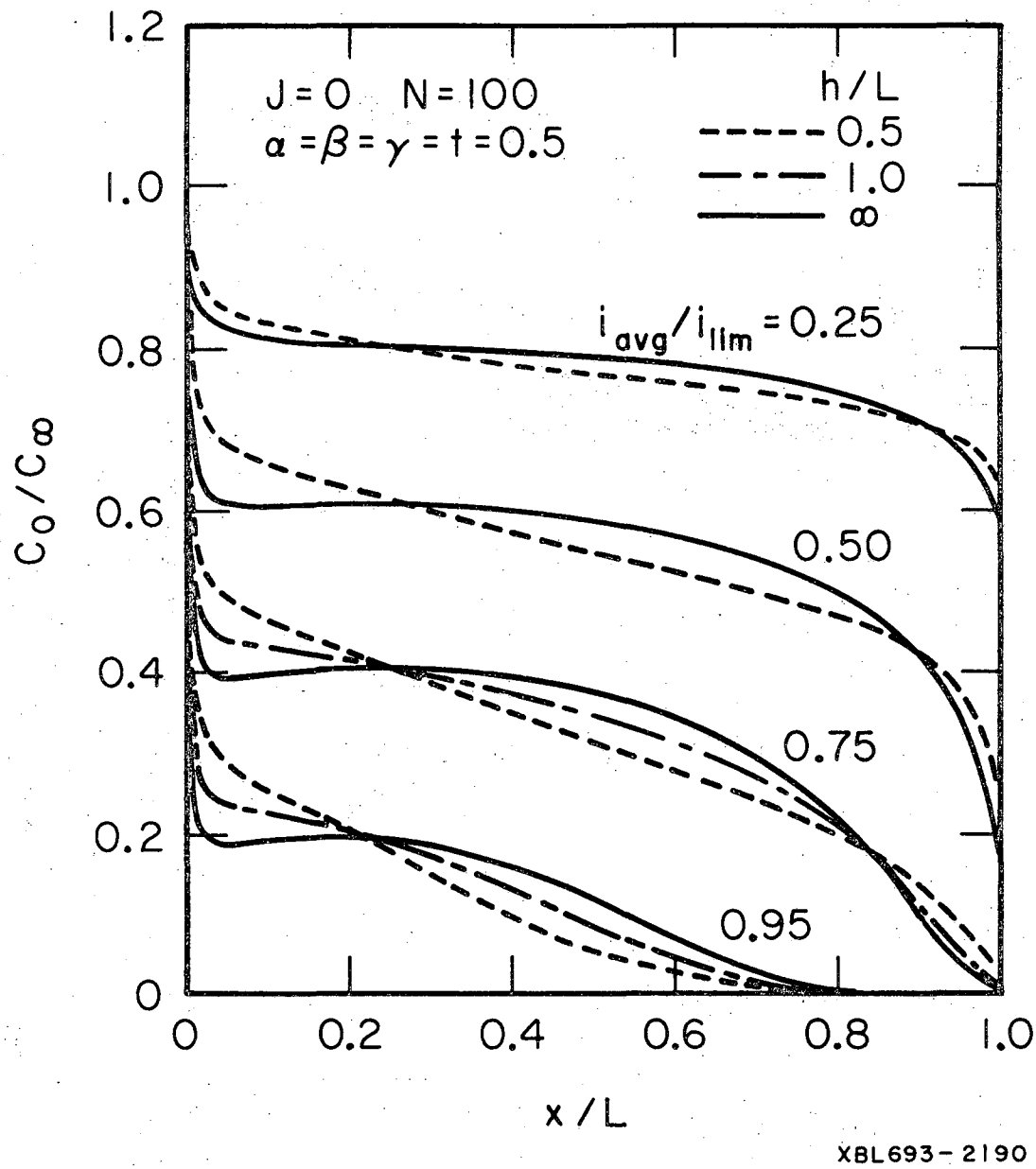

Figure 9. Surface concentration distribution on the cathode for Tafel polarization near the limiting current.

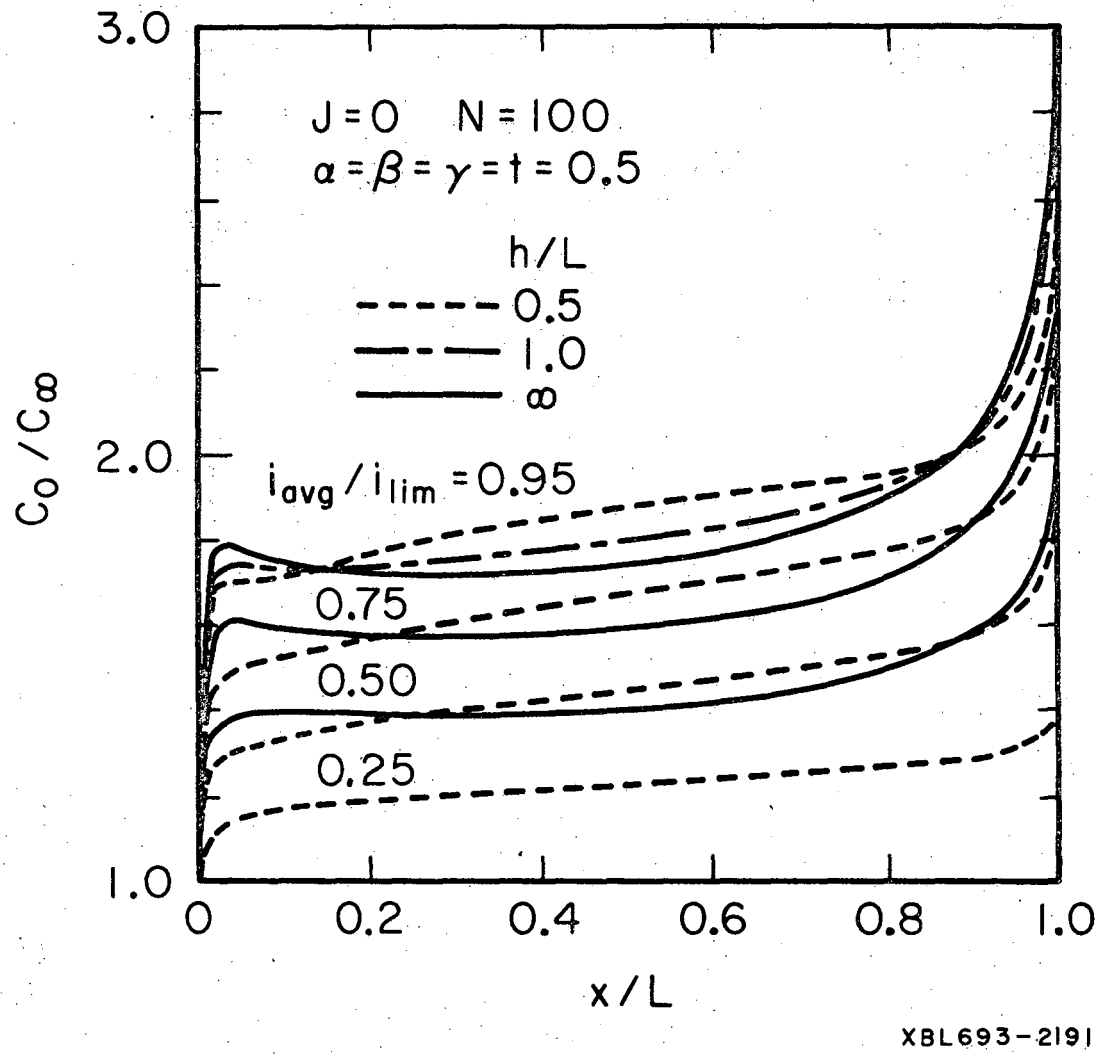

Figure 10. Surface concentration distribution on the anode for Tafel polarization near the limiting current.

Although not shown, current and concentration distributions were calculated for N equal to 5 and 20, for comparable fractions of the limiting current and h/L as discussed above. At the lower values of N, the differences between the current distributions at h/L of 0.5 and infinity were less than 5 and 12 percent on cathode and anode at x/L = 0.5.

Conclusions

A general approach applied previously to flat plate and rotating disk electrodes, has been used to calculate current distributions on two plane, parallel electrodes embedded in the walls of a flow channel. The method of solution takes into account mass transfer effects as well as electrode kinetics and ohmic drop in the bulk region. The same approach should be applicable to other flow geometries if the velocity gradient is known at the electrode surface, and if the potential distribution in the bulk region can be obtained from Laplace's equation.

Based on the above results, the two electrodes can be treated separately if h/L is ten or more. This is also a fairly good approximation for h/L down to 0.5 if the current density (or $(\alpha+\beta)J$ in the case of linear polarization) is relatively small. This assumption greatly reduces the numerical work required to calculate current and concentration distributions on electrodes in flow channels.

Acknowledgment

This work was supported by the United States Atomic Energy Commission.

Nomenclature

c_o	concentration at electrode surface, mole/cm^3
c_∞	bulk concentration of reactant, mole/cm^3
D	diffusion coefficient of reactant or of binary electrolyte, cm^2/sec
F	Faraday's constant, 96,487 coul/equiv
h	height of flow channel, cm
i	normal current density at electrode surface, amp/cm^2
i_{avg}	magnitude of average current density, amp/cm^2
i_{lim}	average limiting current density, amp/cm^2
i_o	exchange current density, amp/cm^2
J	dimensionless exchange current density (see equation 15)
K	complete elliptic integral of the first kind
L	length of electrode, cm
n	number of electrons produced when one reactant ion or molecule reacts
N	dimensionless limiting current (see equation 16)
R	universal gas constant, joule/mole-deg
t	transference number of reactant
T	absolute temperature, deg K
$\langle v \rangle$	average velocity, cm/sec
V	potential of electrode, volt
x	distance along electrode, cm
y	normal distance from electrode, cm
z_i	charge number of species i
Z	see equations 12 and 13

α, β, γ parameters of kinetic expression (see equation 9)

$\Gamma(4/3) =$ 0.89298, the gamma function of 4/3

δ dimensionless average current density (see equation 17)

$\epsilon = \pi L/2h$

η_c concentration overpotential, volt

η_s surface overpotential, volt

κ_∞ conductivity of bulk solution, $ohm^{-1}\text{-}cm^{-1}$

Φ potential in bulk solution, volt

Φ^o potential in bulk solution extrapolated to electrode surface, volt

Φ^* integration constant (see equation 4)

References

1. John Newman. "Engineering Design of Electrochemical Systems." Ind. Eng. Chem., 60 (no. 4), 12-27 (April, 1968).

2. John Newman. "The Effect of Migration in Laminar Diffusion Layers." Intern. J. Heat Mass Transfer, 10, 983-997 (1967).

3. John Newman. "Current Distribution on a Rotating Disk below the Limiting Current." J. Electrochem. Soc., 113, 1235-1241 (1966).

4. John Newman. "The Diffusion Layer on a Rotating Disk Electrode." J. Electrochem. Soc., 114, 239 (1967).

5. W. R. Parrish and John Newman. "Current Distribution on a Plane Electrode below the Limiting Current." J. Electrochem. Soc., 116, 169-172 (1969).

6. H. S. Carslaw and J. C. Jaeger. Conduction of Heat in Solids. Oxford: Clarendon Press, 2nd edition, 1959, p. 30.

7. Andreas Acrivos and Paul L. Chambré. "Laminar Boundary Layer Flows with Surface Reactions." Ind. Eng. Chem., 49, 1025-1029 (1957).

8. Milton Abramowitz and Irene A. Stegun, editors, Handbook of Mathematical Functions. National Bureau of Standards. Washington, D. C., 1964, p. 919.

9. L. V. Kantorovich and V. J. Krylov. Approximate Methods of Higher Analysis. Translated by Curtis D. Benster. New York: Interscience Publishers, Inc., 1959, p. 101.

10. Carl Wagner. "Theoretical Analysis of the Current Density Distribution in Electrolytic Cells." J. Electrochem. Soc., 98, 116-128 (1951).

11. N. P. Gnusin, N. P. Poddubnyĭ, E. N. Rudenko, and A. G. Formin. "Raspredelenie toka na katode v vide polosy v poluprostranstve elektrolita s polyarizatsinnoĭ krivoi vyrazhaemoĭ formuloĭ Tafelya." Elektrokhimiya, 1, 452- 459 (1965).

LEGAL NOTICE

This report was prepared as an account of Government sponsored work. Neither the United States, nor the Commission, nor any person acting on behalf of the Commission:

A. Makes any warranty or representation, expressed or implied, with respect to the accuracy, completeness, or usefulness of the information contained in this report, or that the use of any information, apparatus, method, or process disclosed in this report may not infringe privately owned rights; or

B. Assumes any liabilities with respect to the use of, or for damages resulting from the use of any information, apparatus, method, or process disclosed in this report.

As used in the above, "person acting on behalf of the Commission" includes any employee or contractor of the Commission, or employee of such contractor, to the extent that such employee or contractor of the Commission, or employee of such contractor prepares, disseminates, or provides access to, any information pursuant to his employment or contract with the Commission, or his employment with such contractor.

TECHNICAL INFORMATION DIVISION
LAWRENCE RADIATION LABORATORY
UNIVERSITY OF CALIFORNIA
BERKELEY, CALIFORNIA 94720